LANGMUIR

pubs.acs.org/Langmuir Article

Invisible Bactericidal Coatings on Generic Surfaces through a Convenient Hand Spray

Joey Andrew A. Valinton,[§] Alfin Kurniawan,[§] Ren-Huai Jhang, Christian R. Pangilinan, Che-Hsin Lee, and Chun-Hu Chen*

Cite This: *Langmuir* 2022, 38, 14909–14917 Read Online

ACCESS | Metrics & More | Article Recommendations | Supporting Information

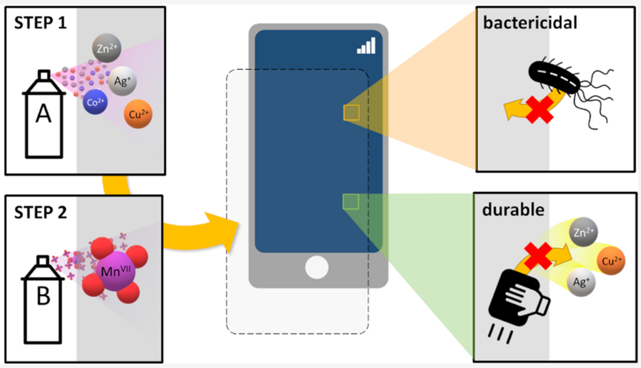

ABSTRACT: Robust antimicrobial coatings featuring high transparency, strong bactericidal activity, and an easy application procedure on generic surfaces can be widely accepted by the public to prevent pandemics. In this work, we demonstrated the hand-sprayer-based approach to deposit complex oxide coatings composed of Co−Mn−Cu−Zn−Ag on screen protectors of smartphones through acidic redox-assisted deposition (ARD). The as-obtained coatings possess high transparency (99.74% transmittance at 550 nm) and long-lasting durability against swiping (for 135 days of average use) or wet cleaning (for a routine of 3 times/day for 33 days). The spray coating enabling 3.14% *Escherichia coli* viability can further be reduced to 0.21% through a consistent elemental composition achieved via the immersion method. The high intake of Cu^{2+} in the coating is majorly responsible for the bactericidal activity, and the presence of Ag^{+} and Zn^{2+} is necessary to achieve almost complete eradication. The success of extending the bactericidal coatings on other typical hand-touched surfaces (e.g., stainless steel railings, rubber handrails, and plastic switches) in public areas has been demonstrated.

■ INTRODUCTION

Stopping global pandemics is an important and urgent task for the scientific community.[1] Significant loss of life and economic activities cause severe impacts on countless families and individuals at every corner. Like all of the pandemics recorded in history, close physical contact and poor disinfection on hand-touched surfaces always lead to the rapid transmission of germs and viruses and ultimately to uncontrollable pandemics.[2,3]

Since smart devices (e.g., cell phones, watches, etc.) have been widely adopted in modern society and among individuals, touch-control panels, usually integrated with monitor displays, have become a major hazard of disease transmission due to frequent touching in daily life. This makes the touch panel of smart devices a "transmission hub" to spread bacteria and viruses on all other surfaces touched by human hands.[4] Therefore, antibacterial coatings on these panels could significantly inhibit disease transmission.[5,6] Nevertheless, such a strategy may only work if the major population is willing to adopt antibacterial coatings on the surface of all kinds of smart devices. This leads to the new criteria for the public to be willing to accept antimicrobial coatings: high transparency, easy operation, generic depositing substrates, and long duration. Low-transparency coatings shield or degrade the visual quality of control display panels, which is almost impossible to convince the public to accept. Complicated coating procedures only compatible with specific substrates would face the same difficult situations. The high durability of coatings, meanwhile, reduces the frequency to repair or reinforce the antimicrobial activities.

Inorganic antimicrobial coatings usually possess a longer duration to most chemicals and mechanical abrasion (e.g., scrubbing and regular cleaning) than their organic counterparts. However, many of the well-recognized inorganic antimicrobial coatings are either too thick to be transparent or too intense in color (e.g., Cu, Ag, or stainless steel surfaces).[7] In this regard, metal-oxide-based ultrathin coatings are a reasonable choice to afford high stability and transparency toward antimicrobial coatings.

Well-reputed deposition methods like chemical vapor deposition (CVD), physical vapor deposition (PVD), and atomic layer deposition (ALD) are simply too complicated for the public.[8−11] Although solution-based deposition techniques generally feature easy operation, typical examples of sol−gel, dip- and spin-coating, and drop-casting still need high-

Received: September 22, 2022
Revised: November 9, 2022
Published: November 23, 2022

https://doi.org/10.1021/acs.langmuir.2c02604
Langmuir 2022, 38, 14909−14917

temperature annealing to consolidate the adhesion of coatings on substrates.[12−15] Public interest may be significantly decreased due to the inconvenience of the additional heating step, which is also forbidden for some soft-substrate devices with low thermal durability. Ambient deposition procedures capable of achieving strong adhesion on generic substrates are therefore highly preferred.[1]

Typically, copper, zinc, and silver cations have intrinsic antimicrobial activities against a wide spectrum of bacteria, viruses, and other microorganisms,[16,17] which can be caused by disruption of cell membranes/coatings[18−20] or oxidative damage due to reactive oxygen species.[21−23] Thus, a thin metal oxide layer containing these three bioactive metals is proposed to provide exceptional antimicrobial activities. In the literature, these cations have been successfully incorporated into oxide-based coatings for bone implants[24,25] and stainless steel substrates.[4] Nevertheless, easy procedures capable of combining all of these cations into one continuous, invisible coating have been too challenging so far.[10,26,27] This would be even more difficult with the criteria of room-temperature conditions on generic substrates.

To address all of the above criteria, the earlier works of acidic redox-assisted deposition (ARD) have been shown to be capable of producing uniform, continuous, and void-free metal oxide thin films with strong adhesion.[28] Such a technique can be applied on diverse substrates such as wood, glass, or metal, among others, through simple immersion onto the deposition mixture in ambient conditions.[7,28−30] Compared to the well-known alkaline precipitation where oxidation states of metal cations remain the same, ARD and the precipitation approaches (ARP) are emerging alternatives uniquely featured with tunable oxidation states, homogeneous multielement distribution, and strong adhesion without the need of thermal annealing. In addition, the ARD oxide coatings can incorporate from two (Co−Mn, Cu−Mn)[7,28,29] to three (Fe−Co−Mn)[28] and up to four (Ag−Ce−Fe−Mn)[30] different metal cations in a single layer. Following the simplicity and versatility of the technique, we propose that ambient-condition ARD is promising to dope all of the antimicrobial active cations in one coating via an intuitive, convenient method for the public, such as using a hand sprayer.

In the present study, we have successfully realized transparent bactericidal coatings via a hand-spray-based approach under ambient conditions for 15 min. The as-generated five-metal oxide coatings exhibit transmittance values of 99.74% with a strong adhesion on screen protectors of smartphones. A high bactericidal activity against *Escherichia coli* (with viability at 3.14%) has been observed. The films exhibit strong durability and retain bactericidal activities against finger swiping and wet cleaning for at least 1 month. The incorporation of Cu^{2+} is responsible for the major activities, while the presence of Ag^{+} and Zn^{2+} is crucial to achieve nearly 100% bactericidal activity, as compared to cases with only Cu^{2+} doping. We further demonstrated the success of realizing this bactericidal coating on other typical hand-touched surfaces (e.g., stainless steel railings, rubber hand rails, and plastic switches) commonly seen in public areas.

■ EXPERIMENTAL SECTION

Hand-Spray-Based Approach. Two solutions were prepared for the hand-spray-based approach. Solution A is mainly prepared by adding 0.04 mmol of cobalt(II) acetate tetrahydrate [$Co(CH_3COO)_2 \cdot 4H_2O$; 98%; Alfa Aesar] in 100 mL of deionized water. The addition of bactericidal metals was done by spiking Solution A first with 0.08 mmol of copper(II) nitrate trihydrate [$Cu(NO_3)_2 \cdot 3H_2O$; 99%; Sigma-Aldrich], then with 0.08 of mmol zinc(II) nitrate hexahydrate [$Zn(NO_3)_2 \cdot 6H_2O$; 98%; ACROS], and lastly with 0.08 mmol of silver nitrate ($AgNO_3$; ≥99.8%; AENCORE). Solution B was prepared by dissolving 0.013 mmol of potassium permanganate ($KMnO_4$; ≥99%; J.T. Baker) in 100 mL of deionized water. These were contained in PET spray bottles ready for the spray coating. The plastic covers of tempered glass screen protector substrates were removed before use, while the stainless steel (5 cm × 5 cm), rubber handrail (∼5 cm × ∼5 cm), and electric switch sample substrates were not subjected to specific cleaning steps. Microscope glass slide substrates were subjected to washing (with soapy water, deionized water, acetone, and isopropanol) and blow-drying prior to use. Indium tin oxide (ITO) substrates were washed (with concentrated nitric acid, water, acetone, and isopropanol), dried, and plasma-treated prior to deposition. For the spray process, Solution A was first sprayed directly onto the substrates at a 90° angle for at most five spray shots, or until the solution predominantly coated the entire surface. This was followed by the spraying of Solution B in the same manner. The substrates were left undisturbed for 15 min. To simulate the potential, direct application on electronics, a damp Kimwipe was used to remove the liquid on the substrates, followed by wiping it dry with another sheet. For multiple coats, the same process above was repeated.

Immersion-Coating Approach. For the immersion method, both Solutions A and B (50 mL for each) were mixed in a 250 mL beaker. Afterward, the substrate (ITO glass) was taped (using a double-sided tape) under a floating object (expanded polystyrene block), with the coating side face-down for direct contact with the precursor solution for a film-growth time of 15 min. The immersion-coated ITO was then rinsed with water and dried under a N_2 stream prior to use. We named this series of immersion-method oxide coatings with an "-IOC" suffix to be distinguished from the spray-coating samples. To create the two-metal oxide coating (CoMn-IOC), only Co^{2+} and MnO_4^- precursors were used in the growth solution. The growth solutions for the cases of three-metal (CoMnCu-IOC) and four-metal (CoMnCuZn-IOC) coatings were prepared by additionally spiking the corresponding cation precursors (0.80 mM each) into the growth solutions of CoMn-IOC. The coating containing all five metals is named CoMnCuZnAg-IOC.

Coating Characterization. The transparencies of the coated glass substrates were measured using a JASCO V-630 double-beam UV−vis spectrophotometer. For the surface analysis, X-ray photoelectron spectroscopy (XPS) measurements were performed using a VG ESCALAB 250 spectrometer measured using an Al Kα source. The microstructural images were taken using an FEI Inspect F50 scanning electron microscope.

Durability Tests. The durability test setup was made by putting a rubber eraser (or a water-wet Kimwipe) under a 100 g weight and placing it over a spray-coated microscope glass slide (see Figure 2a). A swipe was performed by pulling the glass slide out of the weighted setup. The setup was then repositioned over the glass slide again to repeat 100 times. The retained concentrations of Cu, Ag, and Zn were solved following the following equation:

$$\% \text{ concentration} = \frac{I_f - I_i}{I_i} \times 100\% \quad (1)$$

where I_f and I_i are the initial (zero swipes) and final (after 100 swipes) relative intensities of the Cu $2p_{3/2}$, Ag $3d_{3/2}$, and Zn $2p_{3/2}$ peaks in their high-resolution X-ray photoelectron spectra.

Bactericidal Tests. The bactericidal activities of each glass sample were evaluated based on the colony counting method using Gram-negative *Escherichia coli* DH5-α as the model bacteria. All of the experimental procedures were performed following a standard [ISO 14729:2001]. The bacterial suspension was grown in Luria−Bertani (LB) medium (Sigma-Aldrich, pH 7.4) and incubated at 37 °C with gentle shaking for 16 h to reach a stationary phase. Subsequently, aliquots of the bacteria culture were drop-cast onto the sample

https://doi.org/10.1021/acs.langmuir.2c02604
Langmuir 2022, 38, 14909−14917

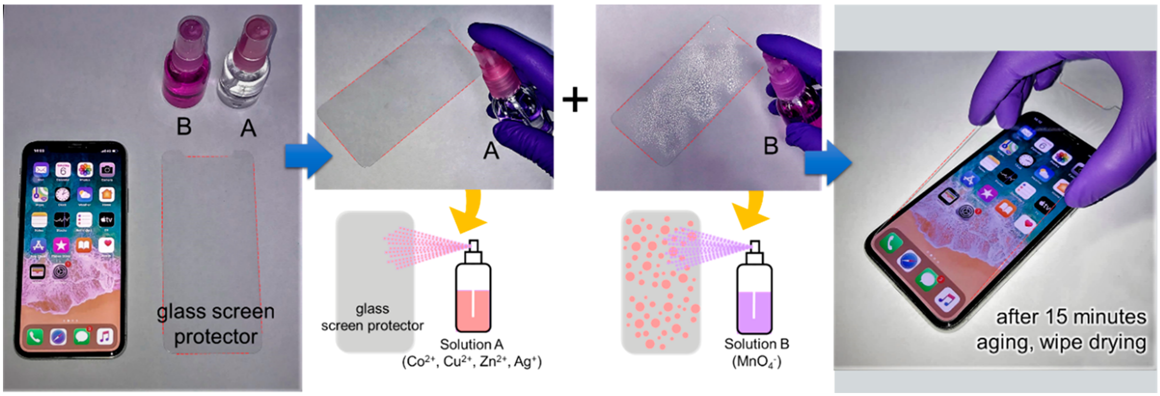

Figure 1. Hand-sprayer coating demonstration on a smartphone screen protector. Solution A (containing Co^{2+}, Cu^{2+}, Ag^{+}, and Zn^{2+}, colorless) and Solution B (containing MnO_4^-, pink) were sprayed consecutively on top of the glass screen protector. After aging at room temperature for 15 min, the solution mixture on the protector was removed to obtain the CoMnCuZnAg oxide coatings.

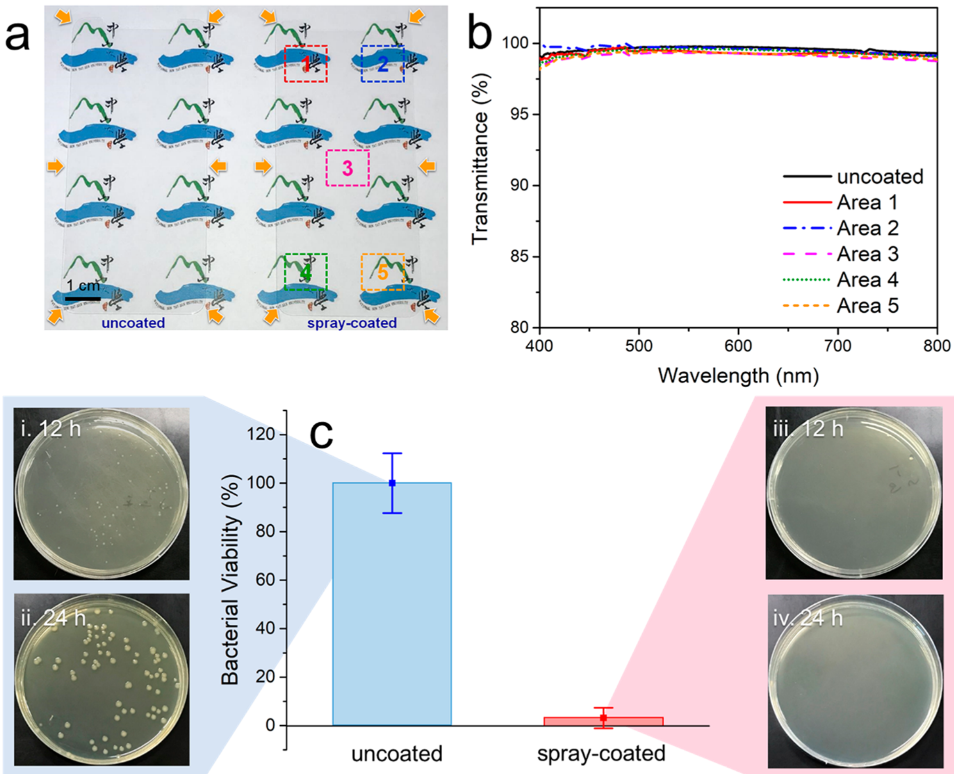

Figure 2. Properties of the hand-sprayer coatings on a smartphone screen protector. (a) Appearance comparison of the uncoated and the spray-coated screen protectors. (b) Visible light transmittance profiles of the locations corresponding to the areas denoted as 1−5 indicated in part a. (c) Bactericidal activity (in percent viability of *E. coli*) of the spray-coated versus the uncoated screen protectors; bacterial cultures show colony growth on uncoated (i and ii) and-spray-coated (iii and iv) ones at different times (12 and 24 h, respectively).

surfaces at a density of 10^4 CFU/mL, followed by incubation at 37 °C for 6 h (12 h for the immersion-coated ITO samples). After incubation, the substrates with the bacterial inoculum were immersed in fresh LB medium and sonicated for 3 min to detach the bacteria adhering to the surface. Aliquots (100 μL) of the diluted bacteria suspension in phosphate buffered saline were then plated on LB agar and incubated at 37 °C overnight. All of the bactericidal tests were performed in triplicate for each sample, and the results are expressed as mean ± standard deviation (SD). The bacterial viability was determined by counting the colony numbers on LB agar plates from appropriate bacterial dilution, and percent viability was obtained according to the following equation:

$$\% \text{ viability} = \frac{N_s}{N_{ctrl}} \times 100\% \quad (2)$$

where N_{ctrl} and N_s represent the average number of bacterial colonies in the uncoated (control) and coated substrates, respectively.

■ RESULTS AND DISCUSSION

The chemical principle of the ARD coating is based on the redox reaction between cobalt(II) acetate (the reductant) and potassium permanganate (the oxidant) in water (eq 3), where the strong oxidative ability of $KMnO_4$ acting on a top surface of generic substrates provides a robust coating adhesion.[28,31]

https://doi.org/10.1021/acs.langmuir.2c02604
Langmuir 2022, 38, 14909−14917

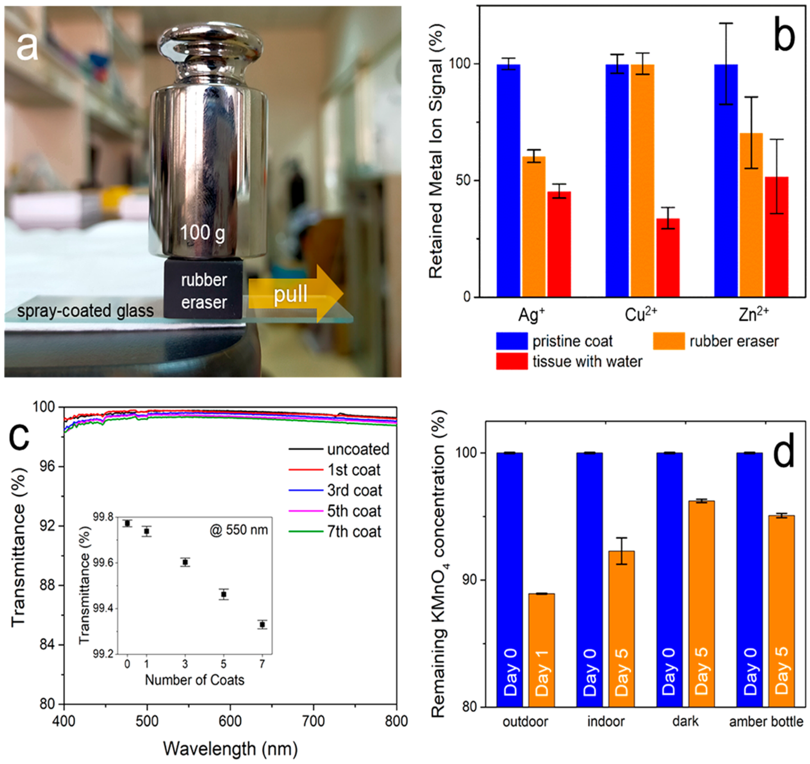

Figure 3. Properties of the hand-sprayer-based coated glass. (a) Procedure for rubbing the coated glass with a rubber eraser with a pressure of 100 g, equivalent to 2.613 kPa and ~5 times the pressure of a finger tapping on a smartphone. (b) XPS results for the percentage of the Ag^+, Cu^{2+}, and Zn^{2+} in the coating after rubbing with a rubber eraser and a wet tissue using the setup in part a. (c) UV transmittance of the glass upon multiple applications of the hand-sprayer coating; inset shows the transmittance values (at 550 nm) being lowered by the increased number of coats. (d) Percentages of $KMnO_4$ remaining in Solution B after exposure to different conditions, based on the absorbance at a 525.5 nm wavelength (the λ_{max} of $KMnO_4$).

$$9Co^{II}(aq) + 3Mn^{VII}O_4^-(aq) + 14H_2O(l) \rightarrow Co^{III}{}_9Mn^{IV}{}_3O_{26}H_{13}(s) + 15H^+(aq) \quad (3)$$

The products of cobalt manganese oxyhydroxide ($Co^{III}{}_9Mn^{IV}{}_3O_{26}H_{13}$, denoted as CMOH) have been shown to be a highly continuous film with a thickness as small as tens of nanometers, enabling high transparency with full surface coverage.[29] The acidic nature of the reaction mixture avoids the occurrence of alkaline precipitation.[32] The oxidant MnO_4^- is most likely to lead to rapid corrosion on the substrates to gain strong adhesion.[28] Meanwhile, the oxyhydroxide layer formation behavior has been observed to be dependent on the counter-anions of the metal precursors, where the mechanism studies show a self-limiting role of acetate anions during the film growth.[28] Hence, the usage of acetate as the counteranion of the Co precursor should enable regulation on the film thickness for the purpose of high transparency.

The incorporation of other foreign cations during the formation of the CMOH coating is known.[28,30] Whereas a redox reaction (eq 3) is fundamental for the deposition, earlier reports have exhibited not only the successful inclusion of oxidizable metal ions like Co^{2+}, Fe^{2+}, and Ce^{3+} through inner sphere intermediates with the anionic oxidant[26] (in this case, MnO_4^-) but also individual inclusion of oxidation-inert metals like Cu^{2+} or Ag^+ in significant amounts. Thus, we doped antimicrobially active cations into CMOH to yield antibacterial coatings.

Hand-Spray-Based Approach. In a typical deposition procedure, two spray solutions are needed. The first solution, denoted as Solution A, is an aqueous mixture containing Co^{2+}, Cu^{2+}, Zn^{2+}, and Ag^+, while the other one, denoted as Solution B, is a $KMnO_4$ aqueous solution. The separation of Co^{2+} and $KMnO_4$ in two different hand sprayers is the key to trigger the deposition only when the two solutions are mixed. The ratio of Co^{2+} to MnO_4^- was kept at 3:1 as the ideal stoichiometric ratio as shown in eq 3, while the concentrations of other metal cations are twice the Co concentrations. We chose tempered glass screen protectors as the main substrates due to their wide use by the public for diverse smartphones.

The hand-sprayer-based procedure starts with spraying Solution A to cover the entire surface of a screen protector, followed by another spraying of Solution B in the same manner. After a 15 min aging under ambient conditions without any heating step, the mixed solutions can be cleaned by washing with a water rinse or wiping with paper until completely dry. Then, a highly transparent and almost invisible coating has been deposited on the substrates, as demonstrated in Figure 1.

The transparency of the hand-sprayer-coated screen protectors is almost identical to that of the uncoated ones (Figure 2a). The optical transmission spectra collected (Figure 2b) from the five different locations show nearly the same transmittance values, suggesting a highly uniform coverage over the entire top surface. The statistical values of transmittance at 550 nm are 99.74 ± 0.17%, just slightly lower than the uncoated ones. Moreover, all of the metals incorporated are present on the coated surface, as analyzed via X-ray photoelectron spectroscopy (XPS, see the Supporting Information, Figure S1).

https://doi.org/10.1021/acs.langmuir.2c02604
Langmuir 2022, 38, 14909−14917

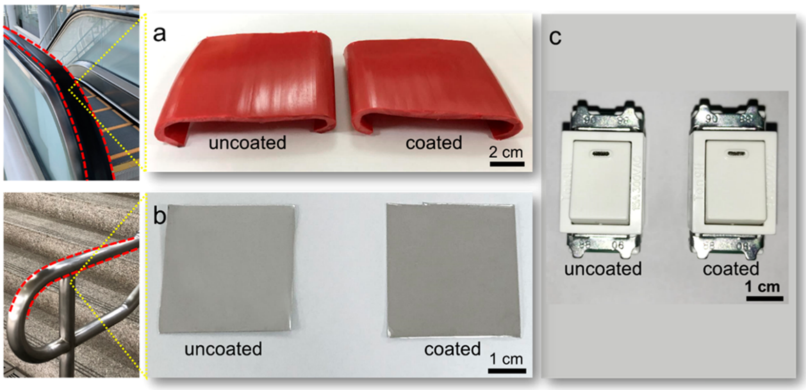

Figure 4. Applicability of the hand-sprayer-based coating on various surfaces. Appearance of the surface before and after spray coating on (a) a rubber surface such as escalator handrails, (b) a stainless steel surface such as stair rails, and (c) an electric switch surface.

To test the bactericidal performance of the hand-sprayer-coated glass as a proof of concept, we performed a bacterial viability test using *E. coli*, a common pathogen seen on smartphones, through incubating a bacterial solution on the surface for a certain amount of time (12 and 24 h, respectively) before transferring to agar plates for colony counting. The hand-sprayer-coated glass shows a significant decrease of viability (3.14 ± 4.22%) compared to the uncoated one (100 ± 12.33%), realizing the immense bactericidal activity (Figure 2c). Such activity is comparable to other bactericidal coatings in the literature as well as those that are commercially available (Table S1). On one hand, the uncoated culture plates (insets of Figure 2c) show live bacteria colonies (white spots) after 12 h (i), which multiplied after 24 h (ii), indicating further bacterial proliferation; on the other hand, almost no sign of bacterial growth is seen in the hand-sprayer-coated glass cultures after 12 h (iii), and they become virtually clean after 24 h (iv). Overall, this proves the bactericidal efficacy of the hand-sprayer-coated surface.

To test the coating durability against swiping, a setup composed of a rubber eraser pressed down by a 100 g weight (corresponding to a pressure of 2.31 kPa) was used (Figure 3a). Pressurized swiping was simulated by pulling the hand-sprayer-coated glass while holding the setup in place. After 100 swipes, the samples show that the retained loadings of Ag and Zn decreased to 60.44% and 44.42%, respectively, while the Cu is highly preserved at 99.04% (Figure 3b). Relating to the average finger swiping pressure of 0.5 kPa,[33] the projected complete removal of Ag, Zn, and Cu should occur after 940, 1321, and 48 300 swipes, respectively. Hence, the bactericidal coating may remain for ∼185 days based on the daily average swiping interactions by the public on mobile devices (2617 swipes a day).[34] In terms of dermal contact, the maximum amount of the metals deposited in a single coat accounts only to 0.014% (for Cu and Zn) and 0.289% (for Ag) of their respective lethal doses (in mg metal/kg body weight), which ensures safety of usage (see the Supporting Information, Table S2). The durable retention of the film is consistent with those of ARD-coated substrates that can resist 100 cycles of peeling-off using adhesive tape[28] as well as coated stainless steel resisting multiple abrasions by a rubber ball.[7] This suggests the excellent adhesion of the ARD-based coating on the substrate regardless of the transparency level and/or thickness.

Meanwhile, the retention of the coating during frequent cleaning/disinfection routines is also essential to inspect.[1] To exhibit this, we replaced the rubber eraser in the setup (Figure 3a) with a water-damped Kimwipe, where the Ag, Cu, and Zn contents decreased by 45.5%, 33.9%, and 51.7%, respectively, after 100 swipes at 2.31 kPa (Figure 3b). According to the World Health Organization (WHO), high-touch surfaces must be disinfected at least three times daily;[35] hence, 100 wipes would be equivalent to ∼33 days of routine cleaning. This means that the antibacterial activities of the hand-sprayer-based coatings may survive under the suggested disinfection routines for a month. Previously, a Cu^{2+}/MnO_4^--based ARD coating on stainless steel exhibited as high as ∼44% leaching of Cu^{2+} upon continuous water exposure for 500 min.[7] These leached ions are argued to result in bacterial cell death through ingestion,[1,6,7] outweighing the slightly compromised durability of the coating. Nevertheless, regulating the release of the metal ions (i.e., introducing other anions that can manipulate dissolution) may prospectively improve the lifetime of the coating. As such, the observed dissolution of metal ions is quite advantageous toward the bactericidal action.

The effect of reinforcing the hand-sprayer-based coating through multiple layering was also studied to observe whether the transparency becomes compromised. Derived from the transmittance graphs (Figure 3c), by repeated layering up to seven times, the transmittance values at 550 nm (the inset in Figure 3c) are still as high as 99.33%. On average, every layer of deposition only decreases by 0.07% of transmittance. Accordingly, zero transmittance would require a more than 1000 cycles of coating, suggesting that the degraded color and image quality in the spray-coated display panels are unlikely to occur. Thus, the hand-sprayer-based approach could be relatively easy to be accepted by the general public.

The chemical stabilities of both spray solutions were inspected by UV−vis spectroscopy. Although Solution A remains highly stable in the tests, $KMnO_4$ in Solution B could undergo gradual self-decomposition upon exposure to light and heat. The loss of the purple color and the presence of dark precipitates indicate a deactivation and may result in an invalid spray solution.[36] Under dark, cool environments, the loss of MnO_4^- is 0.77% per day (Figure 3d), while a loss of 11.07% per day was observed under sunlight. The use of an amber bottle increases the chemical stability of photosensitive $KMnO_4$, as shown by a loss of 0.98% per day (Figure 3d). The projected shelf life of Solution B until full oxidant depletion would be 9 days under sunlight, or 129 days if stored indoors. Nevertheless, the public users must pay attention to the shelf life of Solution B to ensure the quality of the hand-sprayer coating.

https://doi.org/10.1021/acs.langmuir.2c02604
Langmuir 2022, 38, 14909−14917

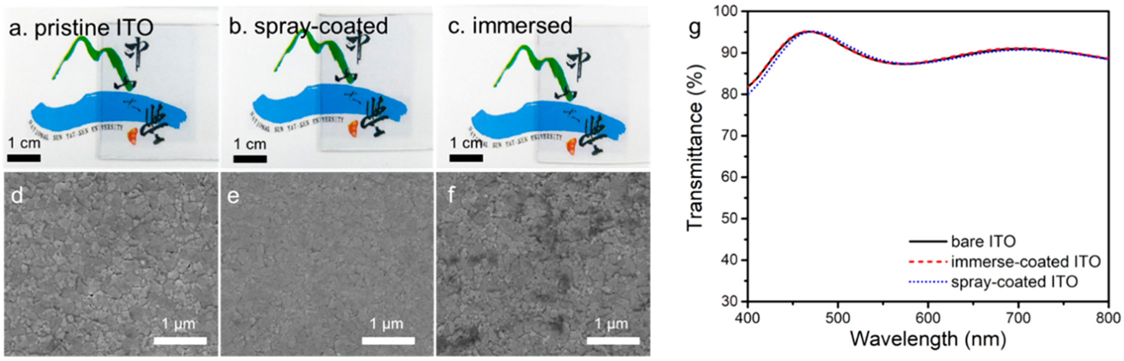

Figure 5. Comparison of the samples prepared by the hand-sprayer-based approach versus the immersion-based approach (i.e., CoMnCuZnAg-IOC) on ITO. Comparison of the physical appearance of the (a) pristine, (b) hand-sprayer-coated, and (c) CoMnCuZnAg-IOC-coated ITO and their corresponding SEM images (d−f, respectively). (g) Transparency results of the three ITO samples.

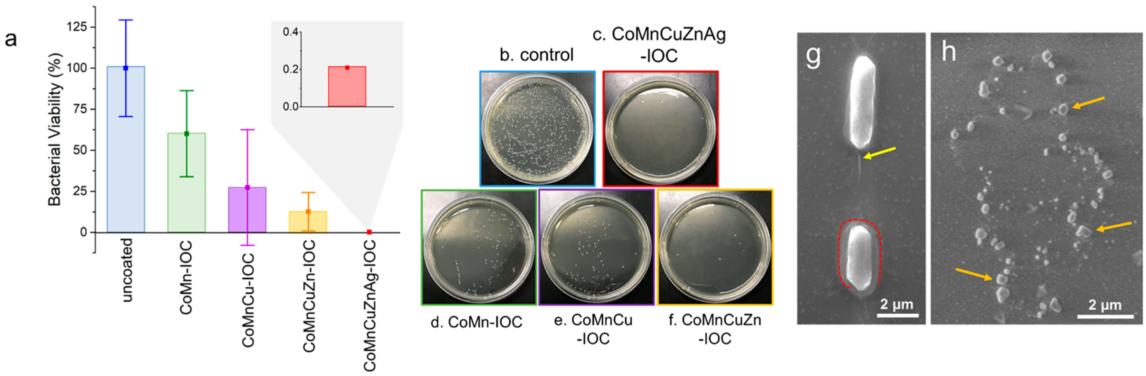

Figure 6. Inhibition of *E. coli* growth in the immersion-grown multimetal oxide films on indium tin oxide glass. (a) Percentage viability on various oxide coatings with different metal combinations; the inset shows the magnified percentage in CoMnCuZnAg-IOC. Culture plates containing the bacterial colonies remaining in the glass after 24 h in the (b) uncoated, (c) CoMnCuZnAg-IOC, (d) CoMn-IOC, (e) CoMnCu-IOC, and (f) CoMnCuZn-IOC samples. The bacterial growth in parts c−e comes from a more diluted culture of recovered live bacteria than those in parts a and b. SEM images of the remnants of bacteria on (g) uncoated ITO substrate, showing the intact flagellum (yellow arrow) and cell membrane (red dashed border), and those on (h) the CoMnCuZnAg-IOC-coated glass showing bacterial fragments (orange arrows).

We further attempt to extend the generality of the antibacterial coatings on various high-risk surfaces in public places and healthcare facilities, including rubber handrails of escalators (Figure 4a), stainless steel objects (e.g., kitchenware, doorknobs, etc., Figure 4b), and finger-touch switches (e.g., light switch and elevator control panels, Figure 4c). These three examples were chosen to represent three typical categories of materials (i.e., rubbers, metals, and plastics) widely used for all kinds of hand-touch surfaces in our modern civilization. The successful deposition of the coating is corroborated by the presence of the multiple cations in the XPS data (Figure S2), revealing the presence of all constituent metals on the tested surfaces. In agreement with the previous test results of the coated glass screen protector, no observable change in visual appearance was seen from these surfaces before and after the hand-sprayer-based coating. These highly transparent features may encourage the public's willingness to apply the ARD antibacterial coatings on surfaces, compared to masking object surfaces by a nontransparent layer (such as Cu foil, antimicrobial paint, and others)[37−39] for antibacterial purposes.

Metals on the Coating and Their Contributions to Bactericidal Activity. In order to understand the contribution of each metal cation to the bactericidal efficacy, we conducted a spike addition-like approach to produce a series of designed compositions as two-metal (Co and Mn), three-metal (Co/Mn/Cu), four-metal (Co/Mn/Cu/Zn), and five-metal (Co/Mn/Cu/Zn/Ag) cases. However, the hand-sprayer-based approach is not reliable enough, since a significant loading uncertainty may be caused from user to user. Alternatively, we adopted an "immersion" route as a much more reliable and repeatable version of preparation to generate samples with well-controlled compositions. In brief, the substrates were floated on the top of the precursor solution mixture (same recipe as mixing Solution A and B) for the same preparation time at room temperature. This method was designed to mimic the limited mass transport of the precursor mixtures on the substrates in the hand-sprayer-based method. These immersion-route-made oxide coatings (i.e., the IOC series) following the spike-addition manner are denoted as CoMn-IOC (two-metal case), CoMnCu-IOC (three-metal case), CoMnCuZn-IOC (four-metal case), and CoMnCuZnAg-IOC (five-metal case).

The transparency of CoMnCuZnAg-IOC is similar to those of both spray-coated samples and the pristine substrates, as recognized by the naked eye (Figure 5a−c). Such an observation remains the same in the microstructural morphology revealed by the scanning electron microscopy images (Figure 5d−f). The transmittance values of the hand-sprayer- and immersion-coated samples at 550 nm (using the pristine glass sample as a blank) are 99.62 ± 0.39% and 98.91 ± 0.20%, respectively (Figure 5g). The XPS data (Figure S3)

https://doi.org/10.1021/acs.langmuir.2c02604
Langmuir 2022, 38, 14909−14917

of CoMnCuZnAg-IOC show composition variations (i.e., elemental ratios among each element) of less than 2.62%, much more reproducible than those produced by the spray method.

By directly conducting *E. coli* viability tests on these IOC samples, the antibacterial activities of each element can be more accurately evaluated. Figure 6a indicates an increase in the order of antibacterial activities of CoMn-IOC (60.14% viability), CoMnCu-IOC (27.34%), CoMnCuZn-IOC (12.59%), and CoMnCuZnAg-IOC (0.21%), which is consistently observed in the bacteria cultures (Figure 6b−f). In CoMn-IOC, the bactericidal effect is contributed by both Co[35] and Mn[40,41] as a bacterial cell membrane disruptor. The spiking of Cu significantly lowers the bactericidal viability by 32.80%, greater than that by the spiking of Zn (14.75%) and Ag (12.38%). If under the same concentrations, Ag and Zn should have intrinsically higher antibacterial activities than Cu.[42−45] But in this case, Cu^{2+} is observed to have higher quantities in the coating than the other two metals (Table S3), which means that the high bactericidal activity should come from the dominant quantity instead of the intrinsic properties. As such, the presence of Zn and Ag, even in much smaller amounts, is necessary to achieve nearly 100% bactericidal activities, hence giving a higher advantage for a multimetal coating.

To determine the direct cause of bacterial cell death on the bactericidal activity of CoMnCuZnAg-IOC, the morphological characteristics of remnant *E. coli* bacteria adhered on the coatings were examined by SEM (Figure 6g,h). The adhered *E. coli* cells on the uncoated ITO have an intact rodlike morphology with a smooth cell membrane (marked with red dashed line) and flagellar filaments[46] (marked by a yellow arrow), characterizing the normal growth of bacteria on this surface (Figure 6g). In stark contrast, the *E. coli* cells attached on the five-metal coating show round or irregular shapes (orange arrows in Figure 6h), which are smaller (average of ∼0.15 μm in diameters) compared to those in Figure 6g (average of ∼3.5 μm) as well as the defective cell membrane and wrinkled surface. Such differences suggest that the rupturing of the bacterial cell membrane could be the main bactericidal action.[16−18,47]

■ CONCLUSIONS

In summary, we have demonstrated a versatile and convenient hand-sprayer-based approach on yielding transparent surfaces that afford potent bactericidal activities. The durability, along with the reapplicability of the coatings without compromising transparency, provides reliable, long-term protection. Compared to the usual options, the features of this coating strategy should integrate well into the common practices of the general public and thus could significantly benefit public healthcare against severe pandemics. Following the proof of concept, we welcome further studies on upgrading this approach toward attaining versatile efficacy against other fomite-transmissible pathogens, including Gram-positive bacteria and viruses (i.e., SARS-CoV-2), for more practical prevention measures against current and future pandemics.

■ ASSOCIATED CONTENT

Supporting Information

The Supporting Information is available free of charge at https://pubs.acs.org/doi/10.1021/acs.langmuir.2c02604.

Bactericidal comparison table, X-ray photoelectron spectroscopy results of the coatings, coating concentration comparison with a lethal dose, and elemental composition data (PDF)

■ AUTHOR INFORMATION

Corresponding Author

Chun-Hu Chen − *Department of Chemistry, National Sun Yat-sen University, Kaohsiung 80424, Taiwan;* orcid.org/0000-0002-3512-6880; Email: chunhu.chen@mail.nsysu.edu.tw

Authors

Joey Andrew A. Valinton − *Department of Chemistry, National Sun Yat-sen University, Kaohsiung 80424, Taiwan;* orcid.org/0000-0002-5244-3765

Alfin Kurniawan − *Department of Chemistry, National Sun Yat-sen University, Kaohsiung 80424, Taiwan;* orcid.org/0000-0003-2867-355X

Ren-Huai Jhang − *Department of Chemistry, National Sun Yat-sen University, Kaohsiung 80424, Taiwan;* orcid.org/0000-0002-8439-5446

Christian R. Pangilinan − *Department of Biological Sciences, National Sun Yat-sen University, Kaohsiung 80424, Taiwan;* orcid.org/0000-0003-3913-7912

Che-Hsin Lee − *Department of Biological Sciences, National Sun Yat-sen University, Kaohsiung 80424, Taiwan*

Complete contact information is available at: https://pubs.acs.org/10.1021/acs.langmuir.2c02604

Author Contributions

[§]J.A.A.V. and A.K. contributed equally. C.-H.C. initiated the concept and provided the funding of this work. J.A.A.V., A.K., and R.-H.J. made the samples and collected the data. J.A.A.V., A.K., and C.-H.C. analyzed the data. C.R.P. and C.-H.L. conducted the biological tests and analysis. J.A.A.V., A.K., and C.-H.C. wrote and edited the paper.

Notes

The authors declare no competing financial interest.

■ ACKNOWLEDGMENTS

We acknowledge the financial support from the Ministry of Science and Technology, Taiwan (Project MOST 109-2628-M-110-001-MY3). We would like to thank D. E. Gracilla and R. E. dela Peña, Jr., for their valuable input in the antibacterial tests.

■ REFERENCES

(1) Huang, H.; Fan, C.; Li, M.; Nie, H.-L.; Wang, F.-B.; Wang, H.; Wang, R.; Xia, J.; Zheng, X.; Zuo, X.; Huang, J. COVID-19: A Call for Physical Scientists and Engineers. *ACS Nano* **2020**, *14* (4), 3747−3754.

(2) *Infection prevention and control of epidemic-and pandemic prone acute respiratory infections in health care.* https://apps.who.int/iris/bitstream/handle/10665/112656/9789241507134_eng.pdf.

(3) Otter, J. A.; Donskey, C.; Yezli, S.; Douthwaite, S.; Goldenberg, S. D.; Weber, D. J. Transmission of SARS and MERS coronaviruses and influenza virus in healthcare settings: the possible role of dry surface contamination. *J. Hosp. Infect.* **2016**, *92* (3), 235−250.

(4) Brady, R. R. W.; Verran, J.; Damani, N. N.; Gibb, A. P. Review of mobile communication devices as potential reservoirs of nosocomial pathogens. *J. Hosp. Infect.* **2009**, *71* (4), 295−300.

(5) Cloutier, M.; Mantovani, D.; Rosei, F. Antibacterial Coatings: Challenges, Perspectives, and Opportunities. *Trends Biotechnol.* **2015**, *33* (11), 637−652.
(6) Imani, S. M.; Ladouceur, L.; Marshall, T.; Maclachlan, R.; Soleymani, L.; Didar, T. F. Antimicrobial Nanomaterials and Coatings: Current Mechanisms and Future Perspectives to Control the Spread of Viruses Including SARS-CoV-2. *ACS Nano* **2020**, *14* (10), 12341−12369.
(7) Huang, H.; Barber, O. W.; Yu, Z.; Park, H.; Hu, X.; Chen, X.; Chen, C.-H.; Hartmann, E. M.; Huang, J. Rub-Resistant Antibacterial Surface Conversion Layer on Stainless Steel. *Adv. Mater. Interfaces* **2022**, *9* (11), 2200251.
(8) Mondschein, J. S.; Callejas, J. F.; Read, C. G.; Chen, J. Y. C.; Holder, C. F.; Badding, C. K.; Schaak, R. E. Crystalline Cobalt Oxide Films for Sustained Electrocatalytic Oxygen Evolution under Strongly Acidic Conditions. *Chem. Mater.* **2017**, *29* (3), 950−957.
(9) Hassan, I. A.; Sathasivam, S.; Nair, S. P.; Carmalt, C. J. Antimicrobial Properties of Copper-Doped ZnO Coatings under Darkness and White Light Illumination. *ACS Omega* **2017**, *2* (8), 4556−4562.
(10) Coll, M.; Napari, M. Atomic layer deposition of functional multicomponent oxides. *APL Mater.* **2019**, *7* (11), 110901.
(11) Pickrahn, K. L.; Park, S. W.; Gorlin, Y.; Lee, H.-B.-R.; Jaramillo, T. F.; Bent, S. F. Active MnOx Electrocatalysts Prepared by Atomic Layer Deposition for Oxygen Evolution and Oxygen Reduction Reactions. *Adv. Energy Mater.* **2012**, *2* (10), 1269−1277.
(12) Stevens, M. B.; Enman, L. J.; Batchellor, A. S.; Cosby, M. R.; Vise, A. E.; Trang, C. D. M.; Boettcher, S. W. Measurement Techniques for the Study of Thin Film Heterogeneous Water Oxidation Electrocatalysts. *Chem. Mater.* **2017**, *29* (1), 120−140.
(13) Smith, R. D. L.; Prévot, M. S.; Fagan, R. D.; Zhang, Z.; Sedach, P. A.; Siu, M. K. J.; Trudel, S.; Berlinguette, C. P. Photochemical Route for Accessing Amorphous Metal Oxide Materials for Water Oxidation Catalysis. *Science* **2013**, *340* (6128), 60−63.
(14) Jia, Q. X.; McCleskey, T. M.; Burrell, A. K.; Lin, Y.; Collis, G. E.; Wang, H.; Li, A. D. Q.; Foltyn, S. R. Polymer-assisted deposition of metal-oxide films. *Nat. Mater.* **2004**, *3* (8), 529−532.
(15) Trotochaud, L.; Ranney, J. K.; Williams, K. N.; Boettcher, S. W. Solution-Cast Metal Oxide Thin Film Electrocatalysts for Oxygen Evolution. *J. Am. Chem. Soc.* **2012**, *134* (41), 17253−17261.
(16) Lemire, J. A.; Harrison, J. J.; Turner, R. J. Antimicrobial activity of metals: mechanisms, molecular targets and applications. *Nat. Rev. Microbiol.* **2013**, *11* (6), 371−384.
(17) Samani, S.; Hossainalipour, S. M.; Tamizifar, M.; Rezaie, H. R. In vitro antibacterial evaluation of sol-gel-derived Zn-, Ag-, and (Zn + Ag)-doped hydroxyapatite coatings against methicillin-resistant Staphylococcus aureus. *J. Biomed. Mater. Res., Part A* **2013**, *101A* (1), 222−230.
(18) Dibrov, P.; Dzioba, J.; Gosink, K. K.; Häse, C. C. Chemiosmotic Mechanism of Antimicrobial Activity of Ag^+ in Vibrio cholerae. *Antimicrob. Agents Chemother.* **2002**, *46* (8), 2668−2670.
(19) Xiu, Z.-m.; Zhang, Q.-b.; Puppala, H. L.; Colvin, V. L.; Alvarez, P. J. J. Negligible Particle-Specific Antibacterial Activity of Silver Nanoparticles. *Nano Lett.* **2012**, *12*, 4271−4275.
(20) Fang, L.; Cai, P.; Chen, W.; Liang, W.; Hong, Z.; Huang, Q. Impact of Cell Wall Structure on the Behavior of Bacterial Cells in the Binding of Copper and Cadmium. *Colloids Surf., A* **2009**, *347* (1), 50−55.
(21) Xi, J.; Wei, G.; An, L.; Xu, Z.; Xu, Z.; Fan, L.; Gao, L. Copper/Carbon Hybrid Nanozyme: Tuning Catalytic Activity by the Copper State for Antibacterial Therapy. *Nano Lett.* **2019**, *19*, 7645−7654.
(22) Raghupathi, K. R.; Koodali, R. T.; Manna, A. C. Size-Dependent Bacterial Growth Inhibition and Mechanism of Antibacterial Activity of Zinc Oxide Nanoparticles. *Langmuir* **2011**, *27*, 4020−4028.
(23) Sehmi, S. K.; Lourenco, C.; Alkhuder, K.; Pike, S. D.; Noimark, S.; Williams, C. K.; Shaffer, M. S. P.; Parkin, I. P.; MacRobert, A. J.; Allan, E. Antibacterial Surfaces with Activity against Antimicrobial Resistant Bacterial Pathogens and Endospores. *ACS Infect. Dis.* **2020**, *6*, 939−946.
(24) Ghosh, R.; Swart, O.; Westgate, S.; Miller, B. L.; Yates, M. Z. Antibacterial Copper-Hydroxyapatite Composite Coatings via Electrochemical Synthesis. *Langmuir* **2019**, *35* (17), 5957−5966.
(25) Geuli, O.; Lewinstein, I.; Mandler, D. Composition-Tailoring of ZnO-Hydroxyapatite Nanocomposite as Bioactive and Antibacterial Coating. *ACS Appl. Nano Mater.* **2019**, *2* (5), 2946−2957.
(26) McGee, S.; Lei, Y.; Goff, J.; Wilkinson, C. J.; Nova, N. N.; Kindle, C. M.; Zhang, F.; Fujisawa, K.; Dimitrov, E.; Sinnott, S. B.; Dabo, I.; Terrones, M.; Zarzar, L. D. Single-Step Direct Laser Writing of Multimetal Oxygen Evolution Catalysts from Liquid Precursors. *ACS Nano* **2021**, *15* (6), 9796−9807.
(27) Kast, M. G.; Cochran, E. A.; Enman, L. J.; Mitchson, G.; Ditto, J.; Siefe, C.; Plassmeyer, P. N.; Greenaway, A. L.; Johnson, D. C.; Page, C. J.; Boettcher, S. W. Amorphous Mixed-Metal Oxide Thin Films from Aqueous Solution Precursors with Near-Atomic Smoothness. *J. Am. Chem. Soc.* **2016**, *138* (51), 16800−16808.
(28) Jhang, R.-H.; Yang, C.-Y.; Shih, M.-C.; Ho, J.-Q.; Tsai, Y.-T.; Chen, C.-H. Redox-assisted multicomponent deposition of ultrathin amorphous metal oxides on arbitrary substrates: highly durable cobalt manganese oxyhydroxide for efficient oxygen evolution. *J. Mater. Chem. A* **2018**, *6* (37), 17915−17928.
(29) Shih, M.-C.; Jhang, R.-H.; Tsai, Y.-T.; Huang, C.-W.; Hung, Y.-J.; Liao, M.-Y.; Huang, J.; Chen, C.-H. Discontinuity-Enhanced Thin Film Electrocatalytic Oxygen Evolution. *Small* **2019**, *15* (50), 1903363.
(30) Zegeye, T. A.; Chen, W.-T.; Hsu, C.-C.; Valinton, J. A. A.; Chen, C.-H. Activation Energy Assessing Potential-Dependent Activities and Site Reconstruction for Oxygen Evolution. *ACS Energy Lett.* **2022**, *7*, 2236−2243.
(31) Suib, S. L. Porous Manganese Oxide Octahedral Molecular Sieves and Octahedral Layered Materials. *Acc. Chem. Res.* **2008**, *41* (4), 479−487.
(32) Yeh, C.-H.; Hsu, W.-Y.; Hsu, C.-C.; Valinton, J. A. A.; Yang, C.-I.; Chiu, C.-c.; Chen, C.-H. Cobalt Iron Oxides Prepared by Acidic Redox-Assisted Precipitation: Characterization, Applications, and New Opportunities. *ACS Appl. Mater. Interfaces* **2021**, *13* (44), 52181−52192.
(33) Hwang, B.-U.; Zabeeb, A.; Trung, T. Q.; Wen, L.; Lee, J. D.; Choi, Y.-I.; Lee, H.-B.; Kim, J. H.; Han, J. G.; Lee, N.-E. A transparent stretchable sensor for distinguishable detection of touch and pressure by capacitive and piezoresistive signal transduction. *NPG Asia Mater.* **2019**, *11* (1), 23.
(34) *Mobile Touches—dscout's inaugural study on humans and their tech*. https://dscout.com/people-nerds/mobile-touches (accessed 2022-06-13).
(35) *Cleaning and disinfection of environmental surfaces in the context of COVID-19*. https://www.who.int/publications/i/item/cleaning-and-disinfection-of-environmental-surfaces-inthe-context-of-covid-19.
(36) Skoog, D. A.; West, D. M.; Holler, F. J.; Crouch, S. R.Applications of Oxidation/Reduction Titrations. In *Fundamentals of Analytical Chemistry*, 9th ed.; Brooks/Cole, 2014; pp 509−534.
(37) Warnes, S. L.; Little, Z. R.; Keevil, C. W.; Colwell, R. Human Coronavirus 229E Remains Infectious on Common Touch Surface Materials. *mBio* **2015**, *6* (6), No. e01697-15.
(38) Govind, V.; Bharadwaj, S.; Sai Ganesh, M. R.; Vishnu, J.; Shankar, K. V.; Shankar, B.; Rajesh, R. Antiviral properties of copper and its alloys to inactivate covid-19 virus: a review. *Biometals* **2021**, *34* (6), 1217−1235.
(39) Hochmannova, L.; Vytrasova, J. Photocatalytic and antimicrobial effects of interior paints. *Prog. Org. Coat.* **2010**, *67* (1), 1−5.
(40) Chata, G.; Nichols, F.; Mercado, R.; Assafa, T.; Millhauser, G. L.; Saltikov, C.; Chen, S. Photodynamic Activity of Graphene Oxide/Polyaniline/Manganese Oxide Ternary Composites toward Both Gram-Positive and Gram-Negative Bacteria. *ACS Appl. Bio Mater.* **2021**, *4* (9), 7025−7033.
(41) Singh, J.; Hegde, P. B.; Ravindra, P.; Sen, P.; Avasthi, S. Ambient Light-Activated Antibacterial Material: Manganese Vana-

dium Oxide ($Mn_2V_2O_7$). *ACS Appl. Bio Mater.* **2021**, *4* (9), 6903−6911.
(42) Ning, C.; Wang, X.; Li, L.; Zhu, Y.; Li, M.; Yu, P.; Zhou, L.; Zhou, Z.; Chen, J.; Tan, G.; Zhang, Y.; Wang, Y.; Mao, C. Concentration Ranges of Antibacterial Cations for Showing the Highest Antibacterial Efficacy but the Least Cytotoxicity against Mammalian Cells: Implications for a New Antibacterial Mechanism. *Chem. Res. Toxicol.* **2015**, *28*, 1815−1822.
(43) Agarwal, A.; Weis, T. L.; Schurr, M. J.; Faith, N. G.; Czuprynski, C. J.; McAnulty, J. F.; Murphy, C. J.; Abbott, N. L. Surfaces modified with nanometer-thick silver-impregnated polymeric films that kill bacteria but support growth of mammalian cells. *Biomaterials* **2010**, *31*, 680−690.
(44) Song, W.; Zhang, J.; Guo, J.; Zhang, J.; Ding, F.; Li, L.; Sun, Z. Role of the dissolved zinc ion and reactive oxygen species in cytotoxicity of ZnO nanoparticles. *Toxicol. Lett.* **2010**, *199*, 389−397.
(45) Burghardt, I.; Lüthen, F.; Prinz, C.; Kreikemeyer, B.; Zietz, C.; Neumann, H.-G.; Rychly, J. A dual function of copper in designing regenerative implants. *Biomaterials* **2015**, *44*, 36−44.
(46) Friedlander, R. S.; Vogel, N.; Aizenberg, J. Role of Flagella in Adhesion of Escherichia coli to Abiotic Surfaces. *Langmuir* **2015**, *31* (22), 6137−6144.
(47) Toyofuku, M.; Nomura, N.; Eberl, L. Types and origins of bacterial membrane vesicles. *Nat. Rev. Microbiol.* **2019**, *17* (1), 13−24.

https://doi.org/10.1021/acs.langmuir.2c02604
Langmuir 2022, 38, 14909−14917